Geodesy and Geodynamics 11 (2020) 135–142

Contents lists available at ScienceDirect

Geodesy and Geodynamics

journal homepage: http://www.keaipublishing.com/geog

Present-day crustal deformation revealed active tectonics in Yogyakarta, Indonesia inferred from GPS observations

Nurrohmat Widjajanti [a], Cecep Pratama [a, *], Parseno [a], T. Aris Sunantyo [a], Leni Sophia Heliani [a], Bilal Ma'ruf [a], Dedi Atunggal [a], Dwi Lestari [a], Hilmiyati Ulinnuha [a], Arinda Pinasti [b], Riska Fajrul Ummi [b]

[a] Department of Geodetic Engineering, Universitas Gadjah Mada, Yogyakarta, Indonesia
[b] Graduate School of Geomatics Engineering, Universitas Gadjah Mada, Yogyakarta, Indonesia

ARTICLE INFO

Article history:
Received 8 October 2019
Accepted 21 February 2020
Available online 12 March 2020

Keywords:
Fault
GPS
Deformation
Strain

ABSTRACT

We investigated the active crustal structure in Yogyakarta, Indonesia, using new and denser Global Positioning System (GPS) data. Deformation rate estimated from five years (2013–2018) of observations on 22 campaign might record broad deformation after the 2006 *M*w7.8 Java tsunami earthquake and postseismic transient due to the 2006 *M*w6.3 Yogyakarta earthquake. We conducted a decomposition method to obtain a short wavelength feature by removing those postseismic deformations from the observation data. The short wavelength pattern revealed active tectonics indicating a combination of E–W dip-slip motion and N–S left-lateral structure. A large maximum shear strain rate (>0.1 microstrain/yr) was estimated along the Opak fault while a large dilatation rate (<-0.1 microstrain/yr) was estimated around the Bantul Graben. The analysis result indicates important implications for crustal dynamics and assessing future seismic hazards potential in the Yogyakarta region.
© 2020 Institute of Seismology, China Earthquake Administration, etc. Production and hosting by Elsevier B.V. on behalf of KeAi Communications Co., Ltd. This is an open access article under the CC BY-NC-ND license (http://creativecommons.org/licenses/by-nc-nd/4.0/).

1. Introduction

Java Island is a home for the volcano and active fault which are geologically influenced by tectonic activities from subducted Australian plate beneath Sundaland block. In general, Java experiences a tremendous compressional strain with postseismic extensional strain due to the 2006 Java Tsunami earthquake [1]. Opak river fault, which extends in the southwest-northeast trend, is a major active fault lies in Yogyakarta Special Region, Central Java (Fig. 1). In the last decade, the Opak fault became a single fault that identified as a major active tectonic deformation [2]. Mt Merapi, which is located in the northern part of Yogyakarta, has a potential geological disaster while the Opak river fault also defines as a segment that could potentially break and bring a catastrophic disaster.

In 2006, a *M*w6.3 earthquake struck Yogyakarta city. Although it was *M*w6.3, the earthquake produced devastated ground shaking in Bantul graben, which considerably amplified by volcaniclastic sediments [3]. About 127,000–160,000 houses were destroyed, 50,000 people were wounded, and another more than 5000 people died mostly found at the southern part of Yogyakarta such as Bantul, Sewon, Imogiri and eastern Yogyakarta city such as Sleman and Klaten [4,5].

Before the Yogyakarta earthquake on May 26, 2006, the Opak river fault was the main fault that should be anticipated [2]. However, the seismic source studies of the 2006 Yogyakarta earthquake suggested different fault line outside Opak river fault [6–8]. Those studies proposed left-lateral strike-slip faulting, which parallels with the Opak river fault but little bit eastward about 10–20 km. Moreover, the aftershock distribution is clearly not aligned with the Opak river fault [3,9]. Thus, there might be an unmapped fault line that active and accumulating stress nowadays. On the other hand, Tsuji et al. [7] also found a vast subsidence

* Corresponding author. Jalan Grafika no 2, Bulaksumur, Yogyakarta, 55281, Indonesia.
E-mail address: cecep.pratama@ugm.ac.id (C. Pratama).
Peer review under responsibility of Institute of Seismology, China Earthquake Administration.

Production and Hosting by Elsevier on behalf of KeAi

https://doi.org/10.1016/j.geog.2020.02.001
1674-9847/© 2020 Institute of Seismology, China Earthquake Administration, etc. Production and hosting by Elsevier B.V. on behalf of KeAi Communications Co., Ltd. This is an open access article under the CC BY-NC-ND license (http://creativecommons.org/licenses/by-nc-nd/4.0/).

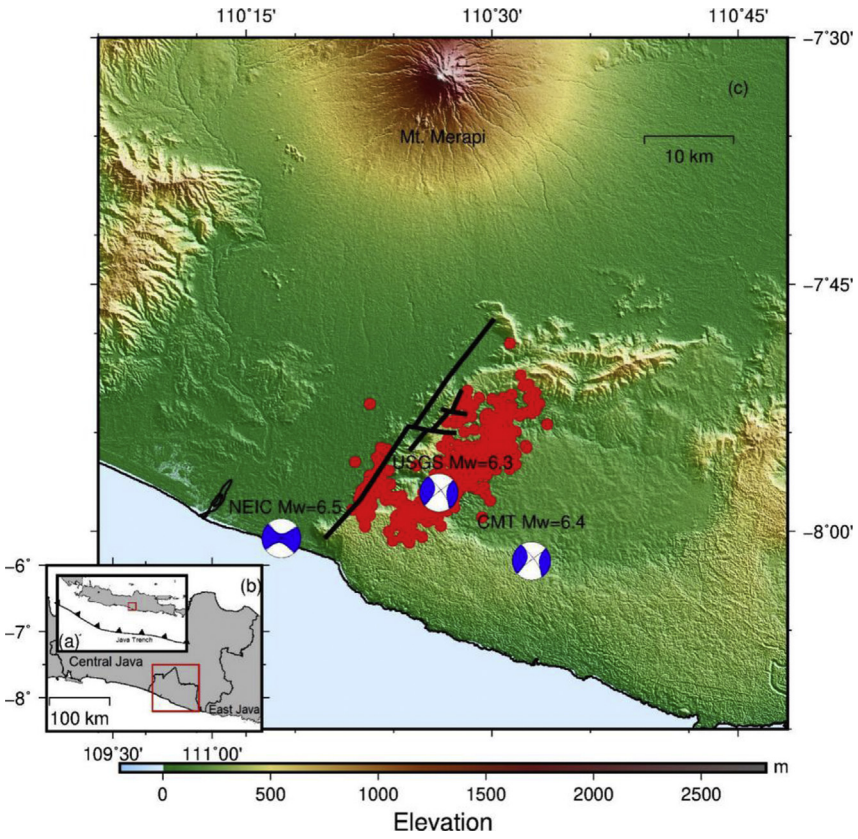

Fig. 1. (a) Red square shows the location of Yogyakarta in Java Island. (b) Red square shows the region of this study bounded by Central Java region and the coast of Southern Java. (c) Tectonic Setting of Yogyakarta region and the epicenter of the 2006 Yogyakarta earthquake are obtained from United States Geological Survey (USGS), National Earthquake Information Center (NEIC) and Harvard Centroid-Moment-Tensor (CMT). Black lines represent identified Opak river fault [3]. Red dots represent relocated aftershock location [9].

region confirmed the Bantul graben in the southward Mt. Merapi and westward Opak fault river inferred from Interferometric Synthetic Aperture Radar (InSAR) data. Those studies indicate that active tectonics in the Yogyakarta region remains poorly understood.

In this study, we present five years of deformation rate based on recent GPS data across the Yogyakarta region. We estimate localized deformation features that lead to a new active fault and emphasize the crustal structure in this region. Also, we calculate strain rate with a denser GPS network since previous studies only use a few data that shown roughly single compressional dilatation rate of western Opak river fault [1]. Here, our geodetic data inferred several unmapped active faults with complex oblique deformation indicates an E–W dip-slip faulting and N–S strike-slip motion. On the other hand, the vertical component reveals a clear boundary between subsidence and uplift on the southwestern Yogyakarta.

2. Data and observation

We analyzed the deformation pattern surrounding the Opak river fault based on five years of geodetic campaign data. This study utilized 17 GPS stations from 2013 to 2016 and 5 GPS stations from 2017 to 2018 along the fault and across the Yogyakarta region. A detailed description of the Opak GPS network in Yogyakarta could be found in separate publications [10]. The data were processed by GAMIT/GLOBK 10.6 software [11] concerning the International Terrestrial Reference Frame 2008 (ITRF2008) [12]. The GLOBK software calculated the deformation rate using the Kalman Filtering method. We obtained the velocities and standard errors of the GPS network from the GLOBK solution, directly.

The GAMIT/GLOBK produces the solution that contained a velocity field with ITRF2008. The estimated velocities were translated into the Sundaland block reference frame to represent the local deformation. It translated using the Euler Pole angular velocity 0.336°/Myr and its position (49.0°N, −94.2°E) defined in the ITRF2000 [13]. In that sense, we transformed our velocity solution from ITRF2008 into ITRF2000 beforehand [14], as had been demonstrated in Gunawan et al. [15]. Hence, we obtained the velocities with respect to the Sundaland block, as shown in Fig. 2.

3. Methods

Yogyakarta region experienced repeated natural hazards such as Mt. Merapi eruptions, shallow damaging Earthquake in 2006 with a wide range of aftershock followed by postseismic deformation [6]. In addition, Yogyakarta also affected by postseismic deformation due to the 2006 Java tsunami earthquake and tectonic activity along the Java subduction zone [16]. The 2012 Indian Ocean earthquake sequences also was recorded at the GPS network in Java Island which was opposite sense with the secular motion in Java Island [17]. Therefore, it may change the deformation pattern in Java Island. Those large and broad range deformation, termed as long-wavelength deformation, may be recorded in our GPS data. Therefore, we intended to extract more local deformation due to inland faults in Yogyakarta. To do so, we applied a moving average filter to obtain the long-wavelength feature that active in the region. Hence, we can subtract the long-wavelength pattern from the original observation. This procedure can be used to detect a short-wavelength deformation from original observation data by removing long-wavelength deformation [18].

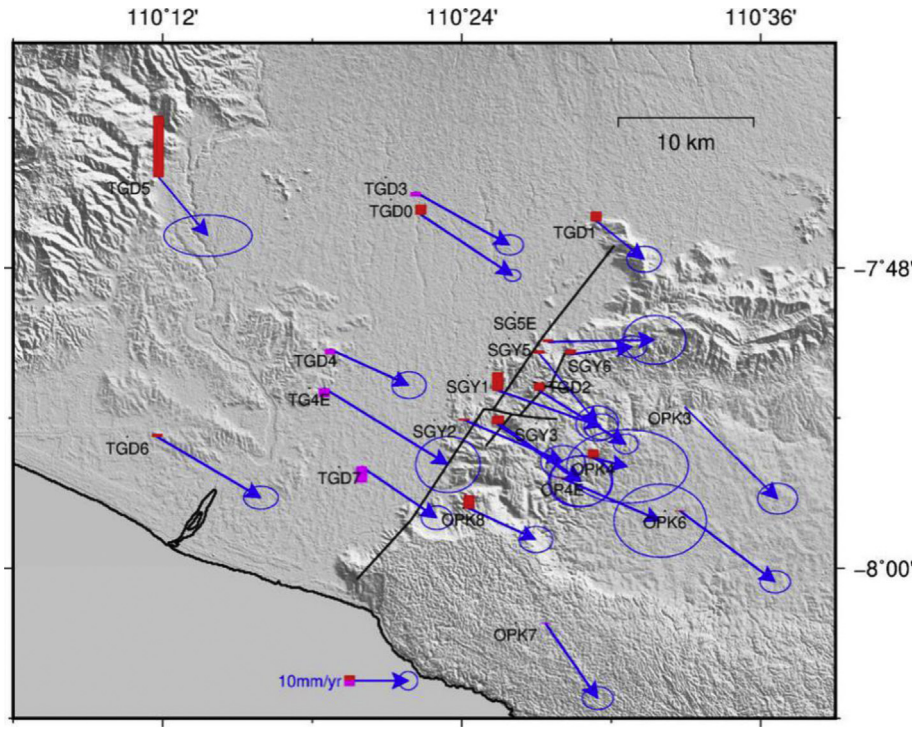

Fig. 2. The GNSS Network in this study. Blue arrows represent the horizontal deformation rate with respect to Sundaland block with one sigma standard errors. Red and magenta bars denote uplift and subsidence, respectively. Black lines indicate the Opak river fault [3].

The moving average filter utilizes the idea of resolving the data by taking the means with homogenous variance. Arithmetic means is applied to determine the linear trend. We tested with several numbers of circular distance from 0.1° to 0.5°. The 0.1° circular distance in moving average filter produced almost zero short-wavelength since the estimated long-wavelength will be the same as original observation in each site. Meanwhile, the 0.5° circular distance in moving average filter produced homogeneous value which cannot capture the long-wavelength pattern from postseismic deformation due to the 2006 Yogyakarta earthquake. Hence, we assumed the optimum radius for moving average filter was calculated from the average distance between each GPS site. The average distance is about 0.24°, thus we performed moving average filter in a radius of 0.24° (approximately 26.64 km) to separate long-wavelength deformation and short-wavelength deformation. The simple equations of moving average can be written as follows

$$\overline{y} = \frac{\sum_1^N y_n}{N} \tag{1}$$

where $\overline{y}$ is the average of horizontal velocities, y_n is the horizontal velocity at designated radius, and N is the number of stations.

After we obtained the deformation rate with respect to moving average filter, as shown in Fig. 3, we are ready to analyze the deformation rate. First, we estimate fault parallel and fault normal velocity based on our latest solution. The fault parallel and normal velocities can be the first signal to see a relative motion for each block assumption. Second, we estimate the strain rate and its derivative to obtain the compression and extensional region. A large strain rate indicates large deformation that would lead to a specific geodynamics process.

In this study, we used grid_strain software with Modified Least Square method to calculate principal strain [19]. Moreover, this method uses scale factor and distance to the nearest point to calculate principal strain. The equation of this method can be written as equation (2) below

$$L = E + \Omega \tag{2}$$

where

$$E = \begin{bmatrix} \frac{\partial}{\partial x}u_x & \frac{1}{2}\left(\frac{\partial}{\partial y}u_x + \frac{\partial}{\partial x}u_y\right) \\ \frac{1}{2}\left(\frac{\partial}{\partial y}u_x + \frac{\partial}{\partial x}u_y\right) & \frac{\partial}{\partial y}u_y \end{bmatrix} \tag{3}$$

and

$$\Omega = \begin{bmatrix} 0 & \frac{1}{2}\left(\frac{\partial}{\partial y}u_x - \frac{\partial}{\partial x}u_y\right) \\ -\frac{1}{2}\left(\frac{\partial}{\partial y}u_x + \frac{\partial}{\partial x}u_y\right) & 0 \end{bmatrix} \tag{4}$$

where L is a tensor, Ω is rotation tensor, E is strain tensor, and u is displacement. Eigenvalues of strain tensor would give us principal strain rate consist of maximum and minimum strain rates represented by λ_1 and λ_2, respectively.

Strain rate analysis can identify tectonic and volcanic activity in the Yogyakarta region. Interpolation that considering scale factor and distance to the nearest point is used to estimate principal strain rate across this region follows the method by Teza et al. [19]. The result of interpolation is useful to represent the activity of a particular area, although it is not the absolute value (e.g. [20]). Based on the estimated principal strain rate, we determine the dilatation rate and the maximum shear strain rate using equations (5) and (6) as follows (e.g. [1,21]).

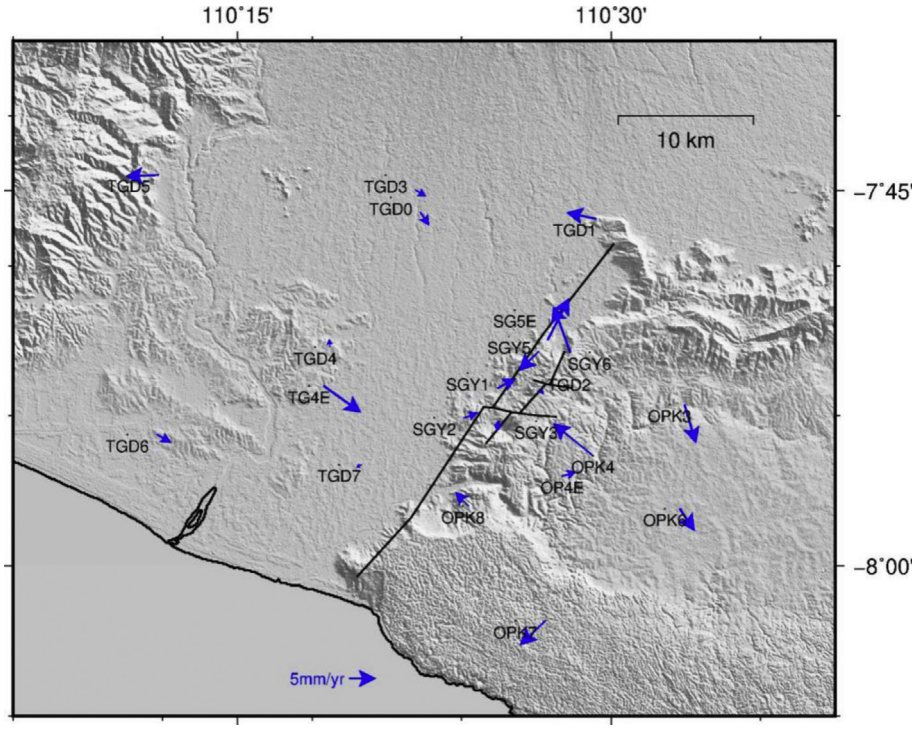

Fig. 3. Corrected velocities with respect to moving average filter around the Opak river fault. Blue arrows represent the horizontal deformation rate with respect to Sundaland block with one sigma standard errors. Black lines indicate the Opak river fault.

$$\varepsilon_{dilatation} = \lambda_1 + \lambda_2 \quad (5)$$

$$\varepsilon_{max\ shear\ strain} = (\lambda_1 - \lambda_2)/2 \quad (6)$$

where $\varepsilon_{dilatation}$ and $\varepsilon_{max\ shear\ strain}$ are dilatation rate and maximum shear strain rate, respectively, with λ_1 is extensional maximum strain rate, and λ_2 is compressional minimum strain rate. The dilatation rate is beneficial to identify dip-slip faulting. Meanwhile, the maximum shear strain rate coincides with strike-slip faulting [1,21].

4. Results and discussion

The estimated displacement rate shows a significant change between the Sundaland block reference frame and short-wavelength pattern after moving average filter (Fig. 3). Most of the GPS trend is moving toward southeast to northeast. Those directions are consistent with the estimated trend for Java island counterclockwise deformation [16]. On the other hand, the detailed quantitative deformation rates (Table 1) show the velocity with respect to the Sundaland block has a larger rate than short-wavelength velocities. In addition, the short-wavelength velocities show heterogeneous motion rather than homogeneous motion on the long-wavelength pattern.

The estimated short-wavelength velocities with its heterogeneity may indicate a multiple fault zone lies across Yogyakarta. Therefore, we calculate fault parallel and normal fault velocity concerning some of the fault hypothesis that we derived from previous studies. First, we suspect a fault on the western Opak river fault that we termed as F1 fault. Studies of Tsuji et al. [7] utilized InSAR analysis suggest a boundary between uplift and subsidence in the southern Yogyakarta region known as Bantul graben. Although most of the vertical GPS data exhibit higher uncertainties than horizontal GPS data, most of our vertical campaign data provide good control except for several stations such as the TGD4 station. Since the error of vertical data on TGD4 is larger than its subsidence rate (Table 1) which may lead to a wrong signal, we do not include vertical information from TGD4 in further analysis. Therefore, we suspect a fault lies between stations that experienced uplift (TGD6, TGD0) and subsidence (TG4E, TGD7) (Fig. 4a). Since TGD6 was applied as a fixed point, we obtained that TGD4 exhibited clear opposite sense motion compared to TG4E for both fault parallel and fault normal velocities. So as shown in Fig. 4a, we suggest the F1 fault, which separated TG4E, TGD7 and TGD4, TGD5, TGD6, TDG0, as an oblique motion combining normal dip-slip and left-lateral strike-slip fault.

Second, we also investigate an identified Opak river fault as a left-lateral strike-slip fault. In Fig. 4c, our GPS data with respect to SGY1 exhibit an apparent left-lateral strike-slip motion in the northern part of Opak river fault. Assuming the Opak fault line as it shows as black lines in Fig. 4c–d, our GPS data shows a consistent left-lateral strike-slip motion in the northern part of Opak river fault (Fig. 4c). However, the Opak fault line in the southern part could be identified as a left-lateral strike-slip motion if we translated the southern Opak fault line 2–3 km to the southeast from its original fault line (Fig. 4d). Moreover, the left-lateral strike-slip motion is more consistent and closer with the focal mechanism of the 2006 Yogyakarta earthquake (Fig. 1). This result probably indicates that Opak river fault affected by east-west trend of slip-partitioning accommodated by the Java megathrust [16]. On the other hand, we obtain a similar normal component movement in the fault normal velocities except for OPK4 site. However, since the uncertainty of horizontal component of OPK4 is considerably large (Fig. 2), we can rule out the probability of dip-slip motion. Therefore, a left-lateral strike-slip motion remains dominant between SGY5, TGD2, SGY3 and OP4E.

Our fault line suggestion coincides with the relocated aftershock distribution of the 2006 *M*w6.3 Yogyakarta earthquake [9]. Previous studies suggest that the aftershock distribution related to the

Table 1
Detailed location of GPS station, deformation rate with respect to (w.r.t.) Sundaland block and deformation rate with respect to moving average filter.

No.	Station Name	Longitude	Latitude	w.r.t Sundaland block (mm/yr)				w.r.t. Moving Average filter (mm/yr)	
				E	N	U	σU	E	N
1	OPK3	110.549	−7.893	15.056	−14.875	0.01	8.71	2.185	−7.412
2	OPK6	110.546	−7.962	15.43	−11.474	0.17	5.57	2.83	−4.226
3	TGD1	110.49	−7.769	7.806	−6.219	17.21	8.15	−5.67	1.169
4	OPK4	110.488	−7.927	5.564	−1.355	15.9	40.81	−7.664	6.272
5	SGY6	110.473	−7.858	9.99	1.264	8.66	5.42	−3.238	8.89
6	OP4E	110.467	−7.94	15.876	−6.844	0.75	23.12	2.649	0.782
7	SG5E	110.458	−7.849	17.299	0.353	5.41	13.04	4.071	7.98
8	OPK7	110.456	−8.037	8.507	−12.172	−0.22	5.86	−4.827	−4.647
9	TGD2	110.452	−7.882	14.054	−8.646	15.3	5.12	0.826	−1.019
10	SGY5	110.452	−7.857	9.443	−11.316	5.18	10.02	−3.785	−3.69
11	SGY3	110.425	−7.904	13.371	−9.345	14.9	16.92	−0.027	−1.611
12	SGY1	110.424	−7.882	16.77	−5.896	34.07	6.82	3.373	1.838
13	SG3E	110.424	−7.904	13.371	−9.345	14.9	16.92	−0.026	−1.611
14	OPK8	110.405	−7.96	10.865	−5.044	24.98	6.85	−2.533	2.69
15	SGY2	110.402	−7.901	15.994	−6.755	2.67	10.61	2.597	0.978
16	TGD0	110.373	−7.764	14.877	−9.859	18.43	2.31	1.606	−2.447
17	TGD3	110.369	−7.75	15.198	−8.529	−7.71	5.27	1.927	−1.118
18	TGD7	110.333	−7.932	12.197	−8.294	−30.16	7.24	−0.956	−0.482
19	TGD4	110.312	−7.854	12.807	−5.806	−9.93	10.97	−0.137	1.47
20	TG4E	110.308	−7.88	20.08	−12.376	−16.96	14.7	7.137	−5.099
21	TGD5	110.197	−7.739	8.011	−9.469	118.61	12.22	−6.268	−0.297
22	TGD6	110.196	−7.912	16.788	−9.875	5.24	7.01	2.594	−1.492

postseismic deformation in the shallow depth due to brittle creep [22]. The hypocenter location frequently coincides with the locking portion of the fault where the stress drop or decrease occurred. On the other hand, a postseismic slip would appear in the region with the stress distribution increase due to an earthquake [23]. Therefore, the locking portion of the fault may not release an aftershock during postseismic while surrounded region release aftershock (Fig. 1). Another study suggests the Baturagung escarpment lineament was derived from remote sensing and fieldwork study based on outcrops deposit characteristic [24], which is consistent with the suggested motion of the fault line in this study.

The third hypothesis of an active fault, which termed as F2, is between OPK6 and OPK3, OPK7 (Fig. 4e). Those three stations exhibited an opposite trend compared to other GPS stations on the left side of the Opak fault river. In that sense, we suspect those three stations may deform affected by another fault. According to OPK3 site as a fixed point, the OPK6 and OPK7 show left-lateral strike-slip sense (Fig. 4e). However, the fault normal velocity at the OPK7 significantly faster than OPK6, which may be indicating a normal dip-slip motion. Therefore, our GPS data suggest another fault line that has similar azimuth of the northern part of the Opak river fault with an oblique motion consist of normal dip-slip and left-lateral strike-slip movement.

In the fault normal velocity analysis, most of the GPS sites toward the Opak river fault suggest compression except for the most western stations (Fig. 4). One possibility is the most western site (TGD5) moving to the east because the moving average filter cannot accommodate the TGD5 site due to short circular distance. To investigate the compression due to fault locking activity, we conduct strain rate analyses to confirm our fault normal and fault parallel velocities trend.

We divide the strain rate analyses into three parts. Firstly, the estimated principal strain rate is shown in Fig. 5. In general, the result indicates the Yogyakarta region experiences E–W contraction and N–S extension. The E–W contraction observed in the whole Yogyakarta region except in the southeastern part exhibits N–S extension. We speculate that our GPS data using moving average filter cannot capture the postseismic deformation due to the 2006 Yogyakarta earthquake resulting in a clear N–S extension where the earthquake occurred (Fig. 1).

Secondly, the estimated maximum shear strain rate provides a high-significance estimate within a grey dashed line, which is shown in Fig. 5a. Although we identified other faults outside the Opak river fault, and a large compressional region observed and confirmed ongoing stress accumulation along the Opak river fault. Moreover, this result coincides with strike-slip motion within fault parallel velocity analysis, which is supported by the focal mechanism of the 2006 Yogyakarta earthquake [3,6]. Thirdly, the estimated dilatation rate provides a high-significance estimate within a grey dashed line shown in Fig. 5b. Its pattern is most likely different from the estimated maximum shear strain where compressional dilatation rate dominant in the northeast side of the Opak river fault. This result is in line with the indicated normal dip-slip faulting by fault normal velocity analysis. Gunawan et al. [1] utilized two GPS data in Yogyakarta suggests a single large dilatation rate. It means the Opak river fault is concluded as dip-slip faulting rather than a strike-slip faulting. However, our denser GPS solution suggests a strike-slip faulting along the Opak river fault and oblique faulting for F1 and F2 fault. On the other hand, a high extensional dilatation rate estimated in the southeast of the Opak river fault, which may indicate the extensional stress due to postseismic deformation of the 2006 Yogyakarta earthquake remains ongoing. Large extension remains detected after Moving Average filter may indicate our GPS network not dense enough to extract postseismic and local earthquake.

In comparison with the subsurface structure imaging, the strike slip faulting along the Opak river fault is consistent with the tomographic imaging derived from P-wave and S-wave velocity perturbation [25]. In addition, the P-wave and S-wave imaging shows different vertical velocity contrast between northern and southern part of the Opak river fault. Moreover, the tomographic imaging also infers the oblique anomaly of extended Ngalang fault which almost align with F2 fault in this study. However, the high resolution of the tomographic imaging only covers the Opak river fault since the study conducted seismic survey around the 2006 *M*w6.3 Yogyakarta earthquake. Hence, densifying seismic survey is necessary to investigate the unmapped fault in Yogyakarta region.

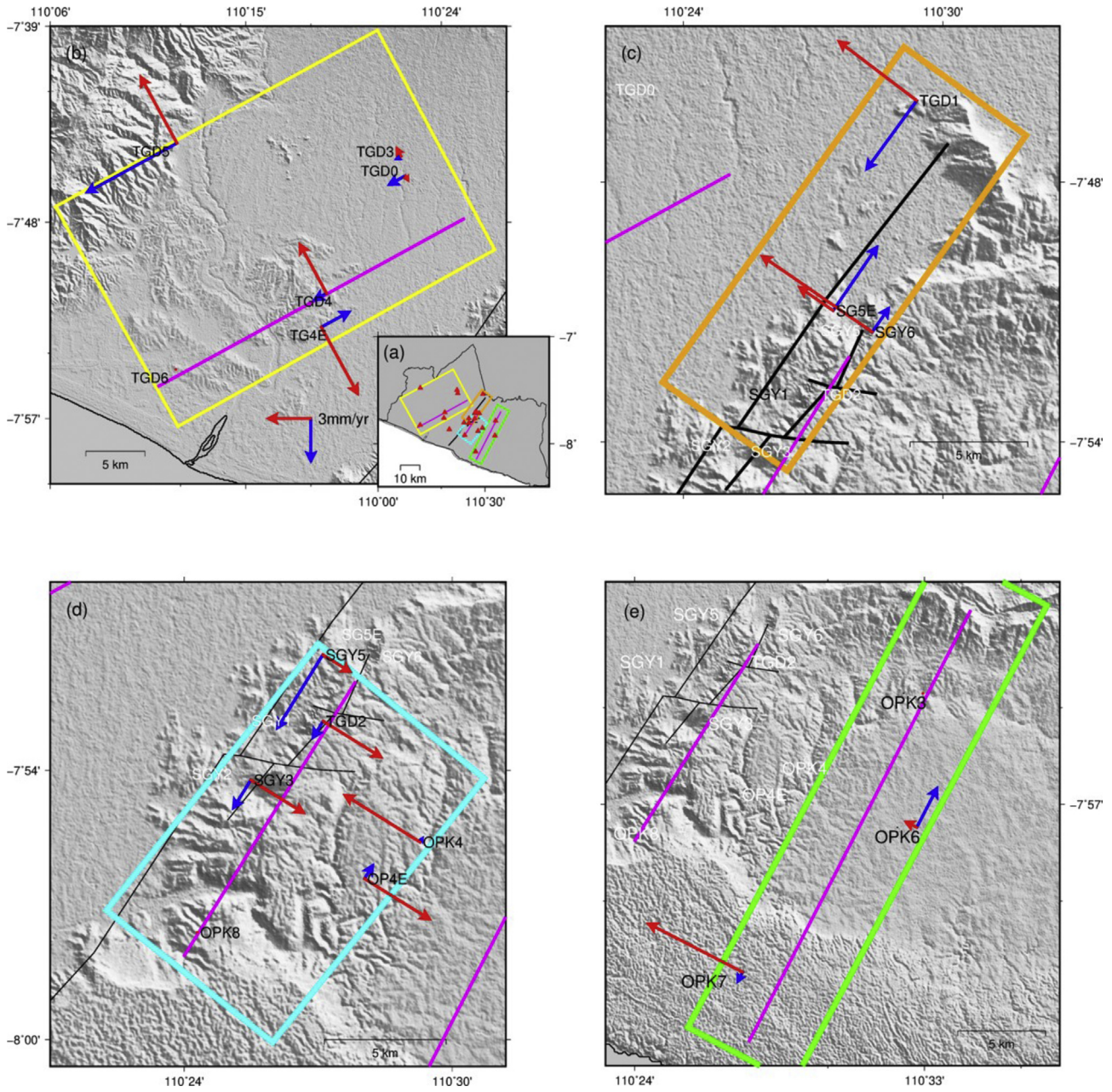

Fig. 4. (a) Each colored frame represents the detailed analysis of fault normal and fault parallel velocity in the next sub-Figure. Red triangles and magenta lines represent GNSS station and new suggested fault, respectively. (b) Magenta lines denote the F1 fault and the velocities with respect to TGD6. (c) Black lines denote the northern Opak river fault and the velocities with respect to SGY1. (d) Black and magenta lines denote old and new southern Opak river faults, respectively. The velocities fixed to OPK8. (e) Magenta lines denote the F2 fault and the velocities with respect to OPK3.

Our finding of the new identified active fault has a strong implication to the earthquake potential and its mitigation in the Yogyakarta region. The 2006 *M*w6.3 Yogyakarta earthquake source lies on one single fault within the Opak fault zone. Therefore, obtaining other fault lines in this region implies a higher possible future earthquake occurrence. However, this study is limited to identify active fault without quantifying the kinematic slip process such as slip rate and locking depth. Those quantitative analyses should be considered in further research by increasing GPS observation density.

5. Conclusions

We studied present-day crustal deformation across the Yogyakarta region based on five years of GPS campaign data. Although our GPS observation is limited, we observed velocity contrast across the faults. Hence, we concluded that active fault in Yogyakarta is not only the Opak river fault. We identified several unmapped active faults on the left and right side Opak river fault, whereas the fault motion has oblique faulting. On the other hand, the northern and southern part of the Opak river fault is consistent with the previous studies of strike-slip faulting, but the southern part is shifted to the east which may be affected by E–W slip partitioning accommodated by the Java subduction process. Finally, these results clearly emphasize the Opak fault zone instead of single Opak river fault in Yogyakarta, Indonesia. Furthermore, those new identified active faults in this region imply the future earthquake potential may increase and need systematic mitigation to prevent casualties.

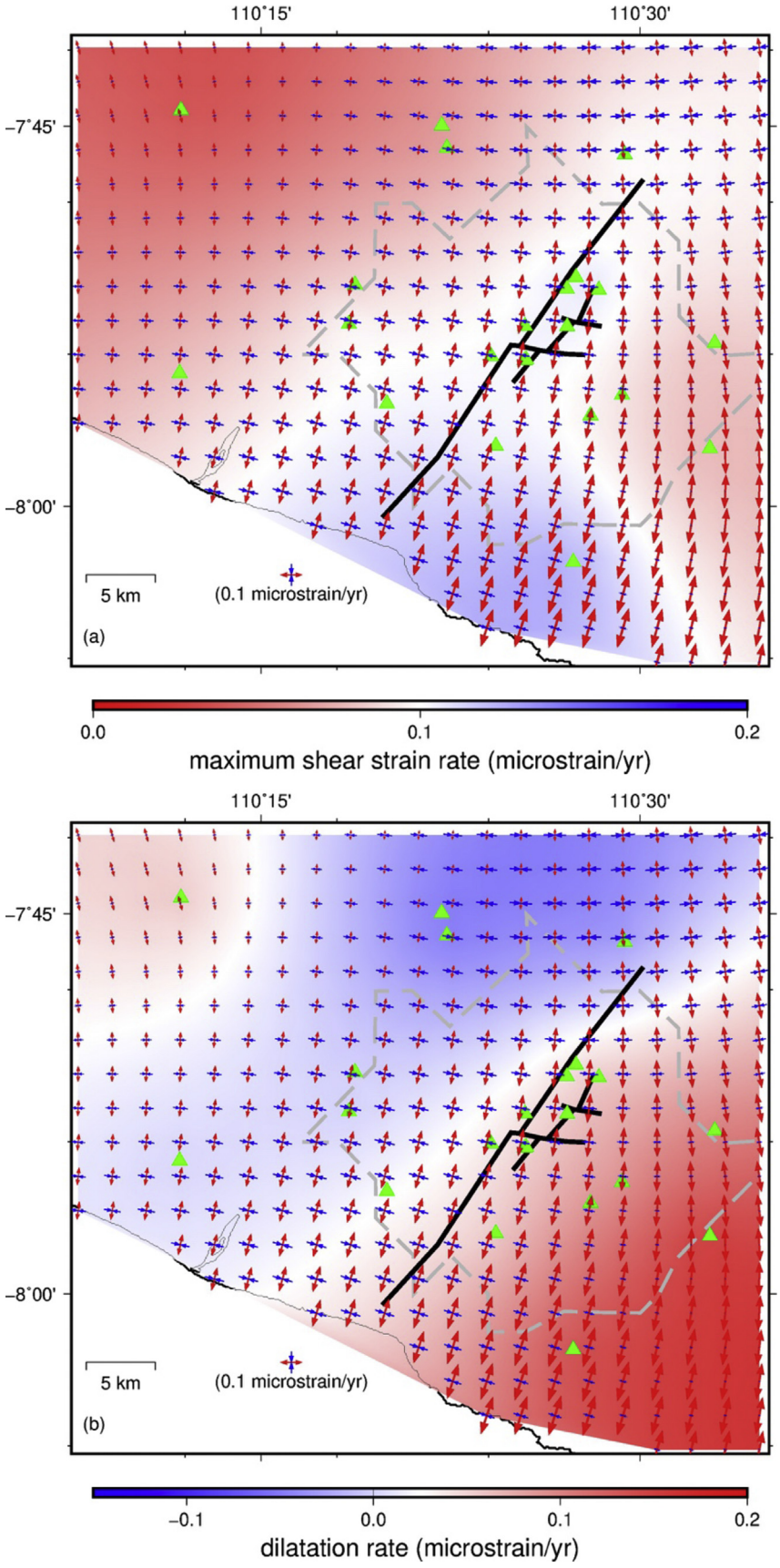

Fig. 5. Black solid lines indicate the Opak river fault [3] while gray dashed lines denote a boundary of high-significance estimate (inside) and mid-significance estimate (outside) of each strain rate. Blue and red arrows represent compression and extension, respectively. The GNSS sites are represented by the green triangle. (a) Principal strain rate vector with maximum shear strain rate. (b) Principal strain rate vector with dilatation rate.

Author contribution

Nurrohmat Widjajanti: Conceptualization, Supervision, Writing-Review & Editing.

Cecep Pratama: Conceptualization, Methodology, Writing-Original Draft.

Parseno: Investigation.

T. Aris Sunantyo: Investigation.

Leni Sophia Heliani: Investigation, Resources.

Bilal Ma'ruf: Investigation, Resources.

Dedi Atunggal: Investigation, Data curation.

Dwi Lestari: Investigation.

Hilmiyati Ulinnuha: Investigation.

Arinda Pinasti: Formal Analysis and Visualization.

Riska Fajrul Ummi: Formal Analysis and Visualization.

Conflict of interest

The authors declare that there is no conflicts of interest.

Acknowledgments

The authors thank the anonymous reviewer and editor for constructive and valuable comments to improve this manuscript. Also, thank Asri Wulandari for providing relocated aftershock distribution. We are indebted to the Geodesy Research Group of Universitas Gadjah Mada for maintaining the GPS observation. This study was partially supported by Universitas Gadjah Mada in the scheme of Final Project Recognition. Most figures were generated by the Generic Mapping Tools [26].

Appendix A. Supplementary data

Supplementary data to this article can be found online at https://doi.org/10.1016/j.geog.2020.02.001.

References

[1] E. Gunawan, S. Widiyantoro, Active tectonic deformation in java, Indonesia inferred from a GPS-Derived strain rate, J. Geodyn. 123 (2019) 49–54.
[2] Sukandarrumidi Rahardjo, Rosidi, Geologic Map of the Yogyakarta Quadriangle, Java, Scale 1:100,000, 1977.
[3] T.R. Walter, et al., The 26 May 2006 magnitude 6.4 yogyakarta earthquake south of mt. merapi volcano: did lahar deposits amplify ground shaking and thus lead to the disaster? Geochemistry, Geophys. Geosystems 9 (5) (2008).
[4] C. G. on Indonesia, Preliminary Damage and Loss Assessment, Yogyakarta and Central Java Natural Disaster: A Joint Report of BAPPENAS, the Provincial and Local Governments of D.I. Yogyakarta, the Provincial and Local Governments of Central Java, and International Partners, 2006.
[5] J. Seeberg, R.S. Padmawati, Redistributing vulnerabilities: house reconstruction following the 2006 central java earthquake, Environ. Hazards 14 (3) (2015) 193–209.
[6] H. Abidin, Deformasi Koseismik Dan Pascaseismik Gempa Yogyakarta 2006 Dari Hasil Survei GPS, Indones. J. Geosci. 4 (4) (2009) 275–284.
[7] T. Tsuji, et al., Earthquake fault of the 26 may 2006 Yogyakarta earthquake observed by SAR interferometry, Earth, Planets Sp. 61 (7) (2009) e29–e32.
[8] C. Sulaeman, Karakterisasi Sumber Gempa Yogyakarta 2006 Berdasarkan Data GPS, Indones. J. Geosci. 3 (1) (2014) 49–56.
[9] A. Wulandari, A. Anggraini, W. Suryanto, Hypocenter analysis of aftershocks data of the Mw 6.3, 27 may 2006 Yogyakarta earthquake using oct-tree importance sampling method, Appl. Mech. Mater. 881 (2018) 89–97.
[10] N. Widjajanti, A.A. Setyawan, T.A. Sunantyo, Parseno, Observation duration and multipath analysis on Yogyakarta Opak fault monitoring stations, in: Proceedings - 2018 4th International Conference On Science And Technology, ICST, vol. 2018, 2018.
[11] T. Herring, R. King, S. McClusky, "GAMIT/GLOBK Reference Manuals, Release 10.6," Cambridge, 2015.
[12] Z. Altamimi, X. Collilieux, L. Métivier, ITRF2008: an improved solution of the international terrestrial reference frame, J. Geodyn. 85 (8) (2011) 457–473.
[13] W.J.F. Simons, et al., A decade of GPS in southeast asia: resolving Sundaland motion and boundaries, J. Geophys. Res. Solid Earth 112 (6) (2007).
[14] Z. Altamimi, X. Collilieux, J. Legrand, B. Garayt, C. Boucher, ITRF2005: a new release of the International Terrestrial Reference Frame based on time series of station positions and Earth Orientation Parameters, J. Geophys. Res. 112 (B9) (Sep. 2007) B09401.
[15] E. Gunawan, S. Widiyantoro, Zulfakriza, I. Meilano, C. Pratama, Postseismic deformation following the 2 July 2013 M w 6.1 Aceh, Indonesia, earthquake estimated using GPS data, J. Asian Earth Sci. 177 (2019) 146–151.
[16] A. Koulali, et al., The kinematics of crustal deformation in Java from GPS observations: implications for fault slip partitioning, Earth Planet Sci. Lett. 458 (2017) 69–79.
[17] C. Pratama, et al., Evaluation of the 2012 Indian Ocean coseismic fault model in 3-D heterogeneous structure based on vertical and horizontal GNSS observation, in: AIP Conference Proceedings, 2018.
[18] A. Meneses-Gutierrez, T. Sagiya, Persistent inelastic deformation in central Japan revealed by GPS observation before and after the Tohoku-oki earthquake, Earth Planet Sci. Lett. 450 (2016) 366–371.
[19] G. Teza, A. Pesci, A. Galgaro, Grid_strain and Grid_strain3: Software packages for strain Field computation in 2D and 3D environments, Comput. Geosci. 34 (9) (2008) 1142–1153.
[20] M. Hackl, R. Malservisi, S. Wdowinski, Strain rate patterns from dense GPS networks, Nat. Hazards Earth Syst. Sci. 9 (2009) 1177–1187.
[21] T. Sagiya, S. Miyazaki, T. Tada, Continuous GPS array and present-day crustal deformation of Japan, Pure Appl. Geophys. 157 (2000) 2303–2322.
[22] H. Perfettini, J.P. Avouac, Postseismic relaxation driven by brittle creep: a possible mechanism to reconcile geodetic measurements and the decay rate of aftershocks, application to the Chi-Chi earthquake, Taiwan, J. Geophys. Res. 109 (B2) (2004) 1–15.
[23] C. Pratama, et al., Transient rheology of the oceanic asthenosphere following the 2012 Indian Ocean Earthquake inferred from geodetic data, J. Asian Earth Sci. 147 (2017) 50–59.
[24] A. Saputra, et al., Determining earthquake susceptible areas Southeast of Yogyakarta, Indonesia—outcrop analysis from structure from motion (SfM) and geographic information system (GIS), Geosciences 8 (4) (2018) 132.
[25] A.D. Diambama, A. Anggraini, M. Nukman, B.G. Lühr, W. Suryanto, Velocity structure of the earthquake zone of theM6.3 Yogyakarta earthquake 2006 from a seismic tomography study, Geophys. J. Int. 21 (6) (2019).
[26] P. Wessel, W.H.F. Smith, R. Scharroo, J. Luis, F. Wobbe, Generic mapping Tools: improved version released, EOS Trans. AGU 94 (45) (2013) 409–410.

Nurrohmat Widjajanti, Associate Professor at Department of Geodetic Engineering, Universitas Gadjah Mada, Indonesia. Her research interests primarily focus on deformation monitoring using GPS data and its mathematical derivation.

Cecep Pratama, Lecturer at Department of Geodetic Engineering, Universitas Gadjah Mada, Indonesia. His research interests primarily focus on tectonic characterization and earthquake physics assessment based on geodetic observation.